Flux-flow instability and its anisotropy in $Bi_2Sr_2CaCu_2O_{8+\delta}$ superconducting films

Z. L. Xiao
Institut für Physik, Universität Mainz, Staudinger Weg 7, D-55099 Mainz, Germany
and Department of Physics and Astronomy, Rutgers University, Piscataway, New Jersey 08855

P. Voss-de Haan, G. Jakob, Th. Kluge, P. Haibach, and H. Adrian
Institut für Physik, Universität Mainz, Staudinger Weg 7, D-55099 Mainz, Germany

E. Y. Andrei
Department of Physics and Astronomy, Rutgers University, Piscataway, New Jersey 08855
(Received 22 July 1998)

We report measurements on voltage instability at high flux-flow velocities in $Bi_2Sr_2CaCu_2O_{8+\delta}$ superconducting films. Current-voltage (I-V) characteristics have been measured as a function of temperature, magnetic field, and angle between the field and the c axis of the sample. Voltage jumps were observed in I-V characteristics taken in all magnetic-field directions and in extended temperature and field ranges. An analysis of the experimental data, based on a theory for viscous flux-flow instability with a finite heat-removal rate from the sample, yielded the inelastic scattering rate and the diffusion length of quasiparticles. Reasonable values of the heat-transfer coefficient from film to bath have been obtained. This theory can also successfully explain the observed scaling behavior $I^*(T,H)=I^*(H)(1-T/T_{co})^{3/2}$ with $I^*(H)\propto 1/(1+H/H_0)^{\alpha}$, where T_{co}, H_0, and α are fitting parameters, determined by the temperature and magnetic-field dependence of the critical current I^* at which the voltage jumps occur. A two-dimensional scaling for the angular dependence of the critical current I^* and the critical voltage V^* associated with the voltage jump has been found and interpreted with a model based on the two-dimensional behavior of this system. [S0163-1829(99)10901-9]

I. INTRODUCTION

Due to the large number of interesting physical phenomena associated with high flux-flow velocities, such as flux-flow instability,[1] crystallization of the vortex system,[2] and self-organized criticality,[3] the dissipation mechanism at high current densities has recently attracted much attention.[4–8] The experimental approach used was to measure current-voltage (I-V) characteristics at high dissipation levels by applying high currents, opposed to experiments at low dissipation levels in investigation of the vortex-glass transition or vortex melting.[9] In low-T_c superconductors, voltage jumps in I-V characteristics originating from different mechanisms were reported in Sn,[10–12] Al,[11,12] In,[12] Mo_3Si,[5] Ta/Ge,[7] Nb,[13] $NbSe_2$,[14] and many other systems.[15,16] In high-T_c superconductors, this voltage jump phenomenon was detected in $YBa_2Cu_3O_{7-\delta}$.[4,6] The inelastic scattering time of quasiparticles can be extracted by interpreting the voltage jumps as a flux-flow instability due to the nonlinear viscosity of the moving vortices as predicted by Larkin and Ovchinnikov (LO).[1] As observed in low-T_c superconductors,[7,11–13] a magnetic-field dependence of the critical current[6] and the critical velocities[6,17,18] has been found in the high-T_c superconductor $YBa_2Cu_3O_{7-\delta}$ and cannot be explained with the original LO theory. The magnetic-field dependence of the critical velocity renders the extracted values of the inelastic scattering rate uncertain. In $YBa_2Cu_3O_{7-\delta}$ (Ref. 6) the temperature and magnetic-field dependence of the critical current I^* was found to scale with a form very similar to that predicted for the depinning critical current I_d in the generalized critical-state model.[19] This scaling behavior of $I^*(T,H)$, in combination with the fact that the voltage jumps also appear in the vortex-glass state,[6,7] led to an interpretation of the voltage jumps in terms of the depinning or self-organized criticality.[20,21] However, such mechanisms can be excluded if the flux-flow behavior (i.e., $V\propto I$) is detected in the I-V characteristics before the voltage jump occurs. Recently we presented observation of voltage jumps at high flux-flow velocities in I-V characteristics of $Bi_2Sr_2CaCu_2O_{8+\delta}$ superconducting films.[8] Due to its low magnetic irreversibility field, the flux-flow behavior was found to appear in a large range of temperatures and magnetic fields. The experimental results for magnetic fields parallel to the c axis of the film were successfully interpreted with the theory of Bezuglyi and Shklovskij (BS), in which the LO model was extended by considering the unavoidable heating of quasiparticles due to the finite rate of removing the power dissipated in the sample.[22] In BS theory, the magnetic-field dependences of the critical current and the critical velocities associated with the voltage jump are understood as a result of the self-heating which leads to a temperature change of the quasiparticles in the films induced by the dissipated power in magnetic fields.

As an extension of our previous work, we present in this paper systematic measurements and detailed discussion of the voltage jump phenomenon in I-V characteristics of $Bi_2Sr_2CaCu_2O_{8+\delta}$ superconducting films, with particular emphasis on the heat transfer from film to bath and the anisotropy of the voltage jumps. We found that the flux-flow instability is the most likely mechanism for the observed voltage jumps, despite the fact that heating affects the experimental results and should be considered in a quantitative analysis. We will also demonstrate that the voltage jumps in

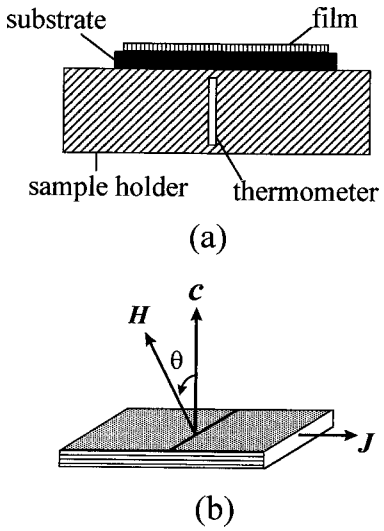

FIG. 1. (a) Schematic of the setup for film, sample holder, and thermometer. (b) Relative direction of current, magnetic field, and c axis of the sample. The definition of the tilt angle θ is also shown.

all magnetic-field orientations have the same origin and the heating effect can be used to probe the anisotropy of this superconductor.

II. EXPERIMENTAL DETAILS

$Bi_2Sr_2CaCu_2O_{8+\delta}$ superconducting films of various thicknesses were prepared by dc sputtering in a pure oxygen atmosphere from a stoichiometric target onto a heated substrate of (100) oriented $SrTiO_3$.[23] As revealed by x-ray analysis, all films were purely c-axis oriented. First the films were patterned into microbridges (length 100 μm, width 10 μm) by photolithography and wet chemical etching. Silver contact pads were evaporated allowing the measurements of I-V characteristics with the standard four-point method. The sample was attached to a copper sample holder, in which a thermometer was mounted, and then placed in a cryostat where external magnetic fields of up to 6 T could be supplied. The sample holder could be rotated to continuously tilt the c axis of the films with respect to the magnetic field, while the current direction was kept perpendicular to the field. Figure 1(a) shows a schematic of the setup for the film, the sample holder and the thermometer. A sketch of the relative directions of the current, the magnetic field and the c axis of the sample is also given in Fig. 1(b). The measurements were performed with rectangular current pulses of 1 s length and an interval time of 3 s between pulses. In order to avoid the destruction of the microbridge, the maximum voltage across it was restricted to below 1 V. (We found that the breakdown electric field for $Bi_2Sr_2CaCu_2O_{8+\delta}$ superconducting films is about 200–300 V/cm.) Four samples were measured and two of them were systematically studied. The sample (A), whose results are presented in this paper, is a 320 nm thick film with superconducting critical temperature (midpoint) $T_c = 85.2$ K and a normal-state electric resistivity of 506 $\mu\Omega$ cm at 100 K. The data of sample B reported in Ref. 8 are presented in this paper for comparison.

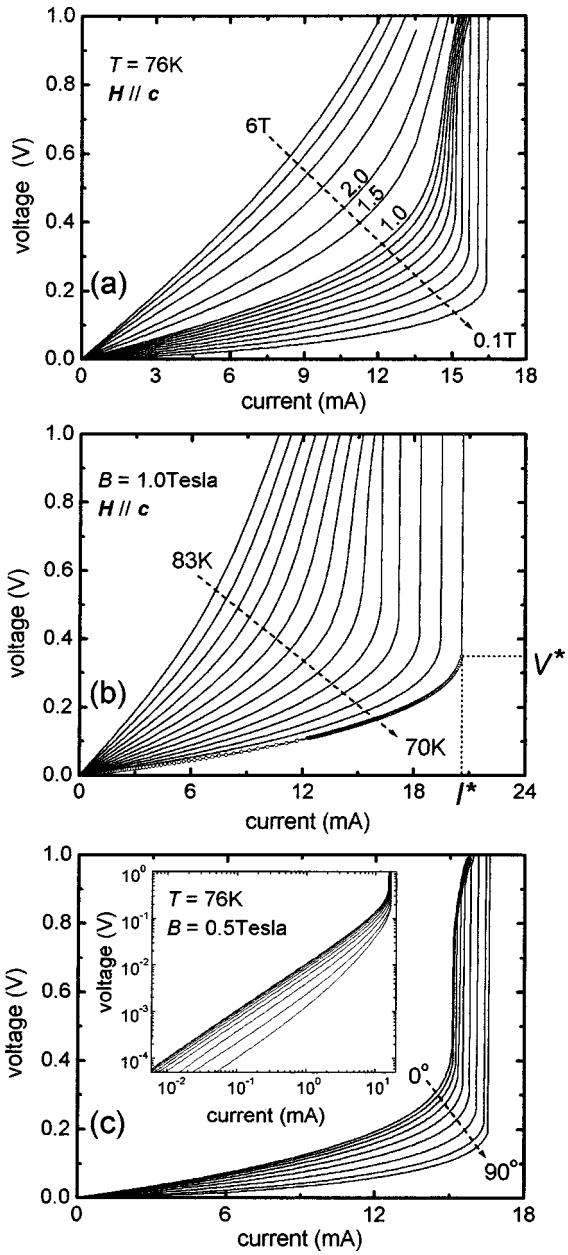

FIG. 2. Current-voltage characteristics taken on a c-axis-oriented $Bi_2Sr_2CaCu_2O_{8+\delta}$ microbridge: (a) at 76 K and magnetic fields (from lower right to upper left) $B = 0.1,0.2,0.3,0.4,0.5,0.6,0.7,0.8,0.9,1,1.5,2,3,4,5,6$ T ($H \| c$). (b) at temperatures 70 K$<T<$83 K with intervals of 1 K and a constant magnetic field of 1 T ($H \| c$). The definitions of the critical current I^* and the critical voltage V^* are indicated by dotted lines. (c) at a fixed temperature of 76 K and magnetic field of 0.5 T for various field orientations $\theta = 0,20,30,40,50,60,70,80,90$ degrees. The inset shows the data in a double-logarithmic scale.

III. RESULTS AND DISCUSSION

A. Voltage jumps in current-voltage characteristics

Figure 2 shows I-V characteristics taken at various temperatures, magnetic fields, and orientations of the field. The data in Fig. 2(a) are taken at 76 K with magnetic fields parallel to the c axis of the film. The field values are given in the caption. Within our experimental resolution the I-V characteristics in magnetic field up to 0.6 T exhibit a discontinuous

voltage jump at a well-defined critical current I^*, which is shifted to lower values with increasing magnetic fields. At high magnetic fields, the I-V curves become more smeared and the voltage jumps disappear in magnetic field greater than 1 T. This behavior is consistent with those found in both conventional superconductors[11–13] and in $YBa_2Cu_3O_{7-\delta}$.[6] The results obtained in a constant magnetic field (1 T, $H\|c$) and various temperatures (from 70 to 83 K in interval of 1 K) are given in Fig. 2(b). As an example for the data at a temperature of 70 K, the definitions of the critical current $I^*$and the critical voltage V^* are indicated by dotted lines. In Fig. 2(c) we present the data obtained at a constant temperature (76 K) and in a constant magnetic field (0.5 T) with various field orientations (θ=0,20,30,40,50,60,70,80,90 degrees). In order to examine the vortex state at lower vortex velocities, the data are plotted again in a double-logarithmic scale in the inset. Obviously, voltage jumps appear in I-V characteristics taken at all magnetic field directions. Both I-V characteristics as well as the critical current I^* and the critical voltage V^* exhibit a strong dependence on the angle between the magnetic field and the c axis of the sample. When the magnetic field is parallel to the c axis, the current I^* necessary to trigger the voltage jump is lower than that for the perpendicular orientation. Conversely, the corresponding critical voltage V^* is much larger for the parallel orientation. This trend of the anisotropic behavior is conserved for all fields

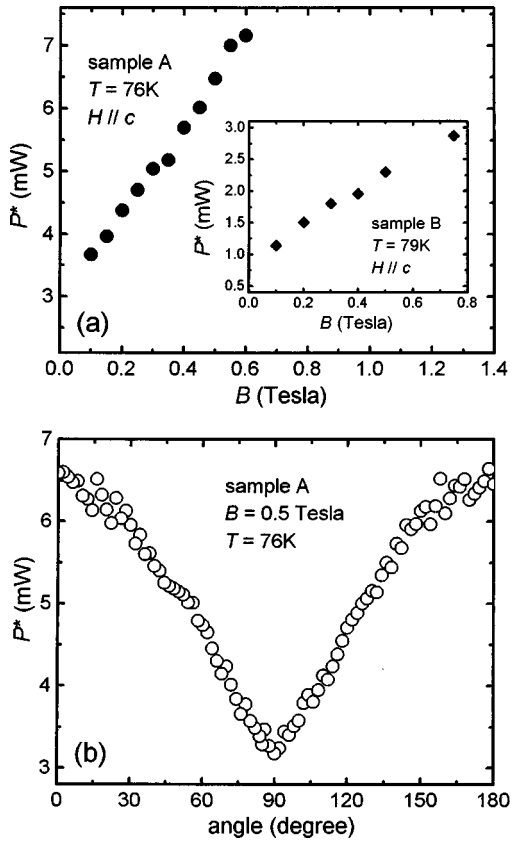

FIG. 3. (a) Dissipated power $P^*=I^*V^*$ just below the voltage jump in sample A at a fixed temperature T=76 K and various magnetic fields. For comparison the data of sample B obtained at 79 K are shown in the inset. (b) Angular dependence of P^* in sample A at a fixed temperature (76 K) and fixed magnetic field (0.5 T).

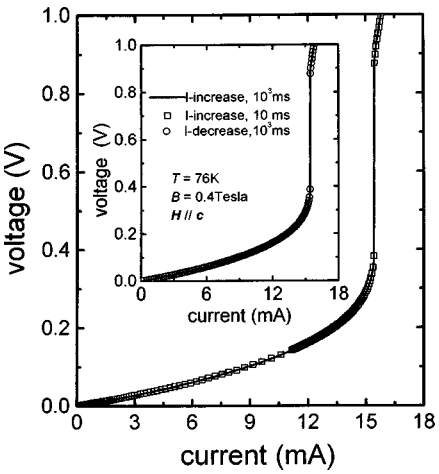

FIG. 4. I-V characteristics at 76 K in 0.4 T ($H\|c$) for various durations t_0 of the current pulses. The comparison of the I-V characteristics taken with increasing and decreasing currents is given in the inset. The solid lines and open squares are the data taken with an increasing current and pulse durations of 1 s and 10 ms, respectively. The open circles represent the results obtained with decreasing currents of $t_0=1$ s.

($B\leqslant 6$ T) and temperature ($T\geqslant 62$K) accessible without damage to the sample in our experiment.

B. Possible mechanisms

As discussed in Refs. 6,8, many mechanisms can cause voltage jumps in I-V characteristics. At high current the power dissipated both in the microbridge and at the current contacts could be high enough to cause a voltage jump due to thermal runaway. There the superconductivity is simply destroyed by excessive Joule heating which leads to an abrupt increase of the sample (microbridge) temperature above the critical temperature T_c. One simple way to exclude this possibility is to check the magnetic-field dependence of the dissipated power $P^*=I^*V^*$ just below the voltage jump at a fixed temperature. If the voltage jump is caused by a thermal runaway, P^* should be independent of the magnetic field. Figure 3(a) and its inset display the dissipated power of sample A at 76 K and sample B at 79 K in various magnetic fields. Clearly, P^* increases with an increasing magnetic field. Figure 3(b) also shows that for a fixed temperature (76 K) and in a fixed applied magnetic field (0.5 T) P^* decreases (from 6.6 to 3.2 mW) for increasing tilt angles (from 0° to 90°) without suppressing the jumps. These results are consistent with the exclusion of thermal runaway as an explanation for the voltage jumps.

Experimental approaches like using short pulses of current,[4,10,24,25] immersing the sample in liquid nitrogen[6] or checking the consistence with independent sets of data[6] can also be used for this purpose. We also measured I-V characteristics for various durations of the current pulse and the corresponding results at 76 K in 0.4 T ($H\|c$) are shown in Fig. 4. Within our experimental resolution the I-V curves for current pulse durations of 10 and 1000 ms are identical. In the inset of Fig. 4 the measurements on the current history are also presented. No difference between the I-V characteristics measured for increasing and decreasing current was observed.

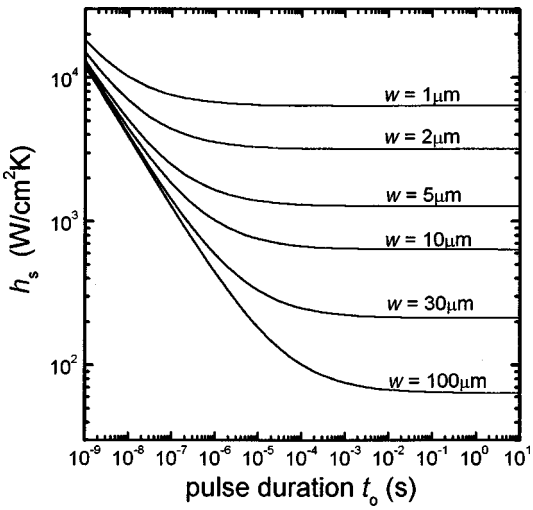

FIG. 5. Pulse duration dependence of the heat-transfer coefficient h_s $[=P/(lw\Delta T_s)]$ for a $SrTiO_3$ substrate, where P and ΔT_s are the dissipated power and the corresponding temperature increase in the sample due to the finite heat removal rate of the substrate, l and w are the length and width of the microbridge, respectively. More details are given in the text. For the calculation we used the thermal constants of $c_p=1$ J/cm^3 K and $D_{\rm th}=0.18$ cm^2/s for $SrTiO_3$.

The pulse duration of the current was expected to influence the heat transfer in the substrate. The temperature increase ΔT_s in the sample due to the finite heat removal rate of the substrate is expressed as:[24] $\Delta T_s=\beta P t_0/\{2l(D_{\rm th}t_0)^{1/2}[4(D_{\rm th}t_0)^{1/2}+w]c_p\}$, where $\beta=4/\pi^{1/2}$, P is the dissipated power in the film, t_0 is the duration of the current pulse, $D_{\rm th}$ and c_p are the heat diffusion constant and the specific heat of the substrate, l and w are the length and width of the microbridge, respectively. In order to simplify the discussion and give the reader a direct look, we plot the pulse duration dependence of the heat-transfer coefficient $h_s[=P/(lw\Delta T_s)]$ for a $SrTiO_3$ substrate in Fig. 5, where $c_p=1$ J/cm^3 K and $D_{\rm th}=0.18$ cm^3/s (Ref. 24) are used. Figure 5 indicates that the influence of the pulse duration t_0 on the heat flow in the substrate depends strongly on the width w of the microbridge. For example, with the same power level to microbridges of $w=100$ and 10 μm, the ratios of the temperature increase ΔT_s for pulse durations of 1 s to 1 μs are about 10 and 1.5, respectively. For microbridges of width w less than 30 μm, the temperature increase ΔT_s is almost independent on the pulse duration of the current if $t_0>1$ ms. In order to reduce ΔT_s, a pulse current duration in the microsecond range should be used.[10,24,25] Substrates like MgO and sapphire with high thermal conductivity can also improve the removal of the dissipated power from the sample.

Despite the fact that the temperature increase in the sample can be minimized by using methods like short current pulses, the dissipated power in the sample cannot be instantaneously removed. The temperature of the sample should exceed that of the bath. The hot-spot effect, which is related to a localized normal hot-spot maintained by Joule heating, has been proposed as an interpretation of the voltage jump phenomenon in some low-T_c superconductors.[15,26] Different physical mechanisms attributed to the voltage jumps may be identified by their characteristic temperature and magnetic-field dependence of the critical current I^* and the critical voltage V^*. Relating to the hot-spot effect, a temperature dependence of the critical current $I^*\sim(1-T/T_c)^{\gamma}$ with $\gamma=1/2$ has been theoretically predicted and was observed in both low-T_c (Refs. 15,26) and high-T_c superconductors.[27] As discussed below, the critical current I^* versus temperature in our $Bi_2Sr_2CaCu_2O_{8+\delta}$ system scales with a power-law form and an exponent $\gamma\approx 3/2$. This temperature behavior is not consistent with the predictions of models based on either the hot-spot effect or crystallization of the vortex system. The shapes of I-V characteristics can also be used to identify the cause of the voltage jumps. For example, the shape shown in Fig. 1 can be used to exclude the channel depinning[14] and hot-spot effect,[15,26,27] which lead in a stepwise form.

In Ref. 6 a scaling behavior for the temperature and magnetic-field dependence of the critical current I^* was observed in $YBa_2Cu_3O_{7-\delta}$. In this paper we will show that the same scaling behavior exists also in $Bi_2Sr_2CaCu_2O_{8+\delta}$ superconducting films and can be explained by BS theory based on the flux-flow instability under the influence of self-heating.[22] This interpretation of the scaling behavior in combination with the observed flux-flow behavior (i.e., $V\propto I$) in I-Vcharacteristics can also be used to exclude the mechanisms of depinning or self-organized criticality.

Thus the voltage jumps observed in our $Bi_2Sr_2CaCu_2O_{8+\delta}$ superconducting films are not caused by the excessive Joule heating itself (thermal runaway), despite the fact that the heating effect influences the experimental results and should be considered in a quantitative analysis. Having excluded the above possible mechanisms, we will analyze our data with the BS theory which extended the LO model on flux-flow instability to include the effect of self-heating. It will be demonstrated that this theory can account for the main feature of the experimental results.

C. Analysis according to the BS extension of the LO theory

According to LO theory, in the flux-flow region the viscous force $f_v\propto v/[1+(v/v_{\rm LO}^*)^2]$ is a nonmonotonous function of the velocity v with a maximum at a critical value $v_{\rm LO}^*=1.02(D/\tau_{\rm in})^{1/2}(1-T/T_c)^{1/4}$, where D is the quasiparticle diffusion coefficient and $\tau_{\rm in}$ is the inelastic scattering time of quasiparticles. Above this critical velocity, the viscous force decreases leading to an even higher velocity accompanied by a still lower viscosity which culminates in a flux-flow instability. This vortex instability appears as a voltage jump in I-V characteristics. The critical voltage V^* associated with the voltage jump is related to the critical flux-flow velocity $v_{\rm LO}^*$ with the following relationship:

$$V^*=Blv_{\rm LO}^*. \tag{1}$$

This equation indicates that the inelastic scattering time of quasiparticles $\tau_{\rm in}$ can be experimentally obtained through measurements of the voltage jumps in I-V characteristics (if the voltage jumps originate from this flux-flow instability). However, as shown in Fig. 6, a magnetic-field dependence of the critical current I^* and the critical velocity v^* is observed in experiments and cannot be explained with the LO model. Recently it has been shown in a theoretical work by Bezuglyi and Shklovskij (BS) that such a magnetic-field dependence

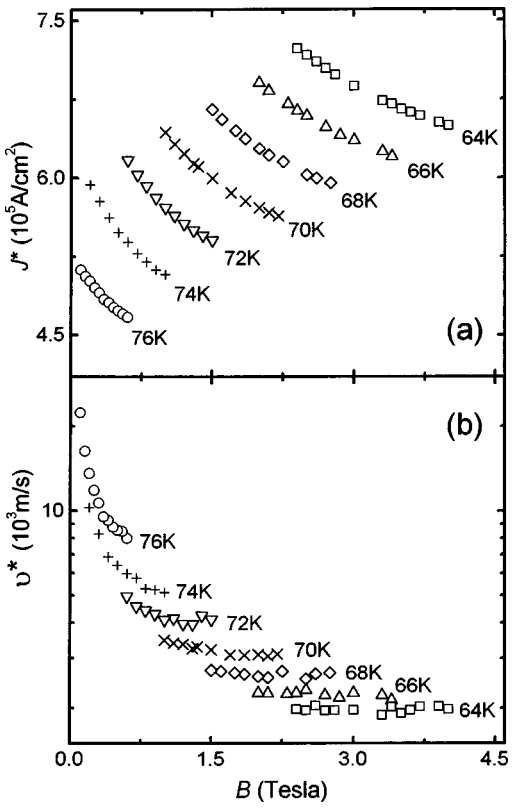

FIG. 6. (a) Magnetic-field dependence of the critical current density J^* and (b) the critical vortex velocity v^* at temperatures as assigned to each curve.

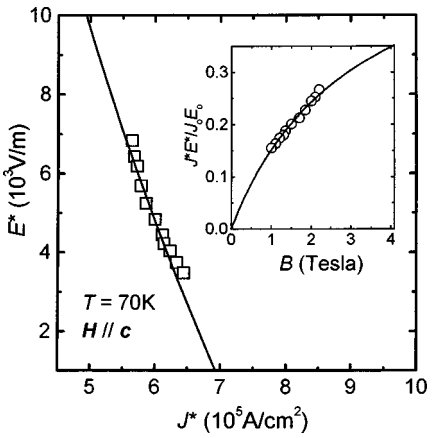

FIG. 7. Relationship of the critical electric field E^* and the critical current density J^* obtained at 70 K and various magnetic fields oriented along the c-axis direction of the sample. The inset shows the corresponding magnetic-field dependence of the normalized power density J^*E^*/J_0E_0. The solid lines are theoretical curves of Eqs. (4) and (5); the symbols represent the experimental data.

can be caused by the unavoidable heating of quasiparticles due to the finite removal rate of the power dissipated in the sample.[22] According to the BS theory, the quasiparticles should have a higher temperature T_q than the experimentally measured temperature T (bath temperature). Their difference is determined by the heat balance equation:

$$T_q - T = d\sigma E^2/h, \tag{2}$$

where $E = vB$ is the electric field, d is the film thickness, and h is the total heat-transfer coefficient from the film (quasiparticle) to the bath. σ is the flux-flow conductivity and its electric-field dependence is expressed as

$$\sigma = \sigma_n(1 - T_q/T_c)^{-1/2}/[1 + (E/E^*_{\mathrm{LO}})^2]B_{c2}/Bf(B/B_{c2}), \tag{3}$$

where σ_n is the normal-state conductivity, $E^*_{\mathrm{LO}} = Bv^*_{\mathrm{LO}}$ is the critical electric field, B_{c2} is the upper critical magnetic field. The function $f(B/B_{c2})$ is related to the vortex core overlap. Solving Eqs. (2) and (3) at the instability point, the magnetic-field dependence of the critical current density J^* $[= I^*/(dw)]$ and the critical electric field E^* $(= Bv^*)$ at a fixed bath temperature are given by

$$J^*/J_0 = 2\sqrt{2}t^{3/4}(3t-1)^{1/2}/(3t+1), \tag{4}$$

$$E^*/E_0 = (1-t)(3t+1)/[2\sqrt{2}t^{3/4}(3t-1)^{1/2}], \tag{5}$$

with $t = [1 + b + (b^2 + 8b + 4)^{1/2}]/[3(1+2b)]$ and $b = B/B_T$. The introduced normalizing current density J_0 and electric field E_0 are temperature dependent, but independent of the magnetic field and are expressed as

$$J_0 = 2.62\sigma_n/e_0(D\tau_{\mathrm{in}})^{-1/2}k_B T_c(1 - T/T_c)^{3/4}, \tag{6}$$

$$E_0 = 1.02B_T(D/\tau_{\mathrm{in}})^{1/2}(1 - T/T_c)^{1/4}, \tag{7}$$

here e_0 is the electron charge and k_B is the Boltzman constant. The characteristic magnetic field $B_T = 0.37k_B^{-1}e_0h\tau_{\mathrm{in}}/\sigma_n d$ separates the regions where the influence of the self-heating is of minor and of major importance for the flux-flow instability.

Equations (4) and (5) are the parametric form of the corresponding E^* and J^* taken in various magnetic fields at a fixed bath temperature. If the voltage jumps in I-V characteristics of the film originate from the flux-flow instability, the relationship between J^* and E^* should follow Eqs. (4) and (5). A comparison of the theory and our experimental data obtained at 70 K, as shown in Fig. 7, yields a satisfactory agreement. By fitting the data taken at various temperatures we obtain the corresponding values of J_0 and E_0 which are given in the inset of Fig. 8(a). Both J_0 and E_0 decrease with increasing temperature and are consistent to the temperature dependence of J_0 and E_0 reported in Ref. 8.

Following the approach used in Ref. 22, we need to determine B_T to obtain the time τ_{in} of inelastic quasiparticle scattering. B_T can be obtained by fitting the experimental data with the magnetic-field dependence of the normalized power density $J^*E^*/J_0E_0 = (1-t)$ derived from Eqs. (4) and (5). The inset of Fig. 7 shows these experimental data and the fitted curve used to extract B_T. The theoretical curve gives a good fit to the experimental data. Values of B_T extracted at various temperatures are plotted in Fig. 8(a). A strong temperature dependence is observed. Based on the BS theory we can extract the inelastic quasiparticle scattering rate $1/\tau_{\mathrm{in}}$ from Eqs. (6) and (7) using the determined J_0, E_0, and B_T. The corresponding results for sample A are presented in Fig. 8(b). For comparison the data of sample B, which were presented in Ref. 8, are also shown in this figure.

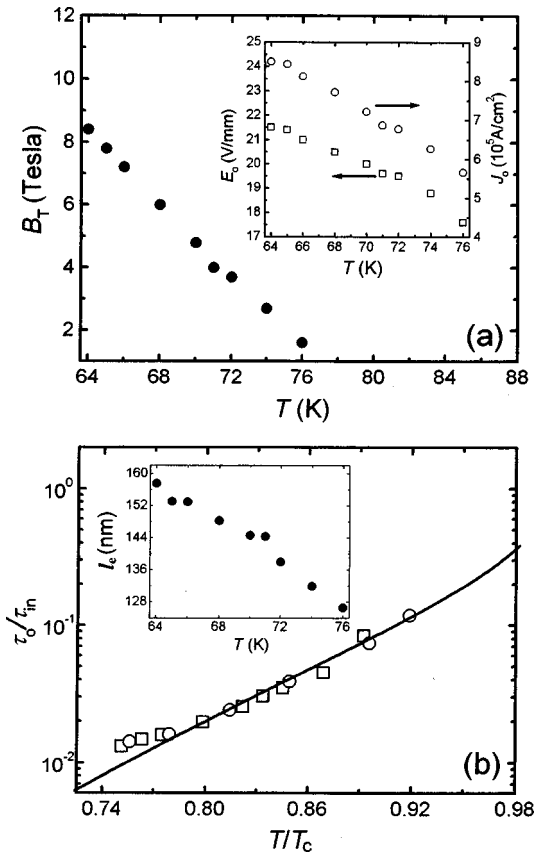

FIG. 8. (a) Characteristic magnetic field B_T versus temperature. The values of E_0 and J_0 obtained by fitting the data of the critical electric field E^* versus the critical current density J^* at different temperatures with Eqs. (4) and (5) are given in the inset. (b) Temperature dependence of the inelastic scattering rate $1/\tau_{in}$. The open squares and open circles are the experimental results of samples *A* and *B*, respectively. The solid line is a fit of Eq. (8) with $1/\tau_0 = 1.71\times10^{12}$ s^{-1} and 1.22×10^{11} s^{-1} for samples *A* and *B*. The inset shows the diffusion length l_e of quasiparticles obtained at various temperatures.

Despite the considerable difference of the absolute values, the temperature dependence of $1/\tau_{in}$ is almost the same in both samples. If $1/\tau_{in}$ is dominated by the inelastic electron-electron scattering, it will be related to the thermally excited quasiparticle density n_q which is proportional to $\exp(-2\Delta/k_BT)$, where $\Delta = 1.76(1-T/T_c)^{1/2}$ stands for the superconducting gap.[4] Thus the temperature dependence of $1/\tau_{in}(\propto n_q^2)$ is expected to be

$$1/\tau_{in} = 1/\tau_0 \exp(-4\Delta/k_BT), \tag{8}$$

where $1/\tau_0$ is the extrapolated value of $1/\tau_{in}$ at T_c. The experimental data at high temperatures can be fitted with Eq. (8), shown in Fig. 8(b) as a solid line, and the extracted values for $1/\tau_0$ are 1.71×10^{12} s^{-1} and 1.22×10^{11} s^{-1} for samples *A* and *B*, respectively. These values are comparable to those determined for $YBa_2Cu_3O_{7-\delta}$.[18] However, the higher electric resistivity in the normal state of sample *A* corresponds to a lower electron density which implies that the corresponding value of $1/\tau_0$ should be lower than that in sample *B*, if electron-electron scattering dominates. Obviously, more theoretical and experimental work, especially in high-T_c superconductors with controlled oxygen content, are needed here.

The diffusion length $l_e = (D\tau_{in})^{1/2}$ plays an important role in BS theory. It must be larger than the core size, in order for the excitations to leave the core, and larger than the intervortex distance to get spatial homogeneity. The values of the diffusion length calculated from Eq. (6) using the extracted J_0 are presented in the inset of Fig. 8(b). It decreases with increasing temperature like in sample *B* (cf. Fig. 4 of Ref. 8). Clearly, it is not only larger than the vortex core size (typically 10 nm) but also larger than the intervortex distance (about 50 nm in a magnetic field of 1 T). The heat-transfer coefficient obtained for sample *A* varies from 286 W/cm^2 K at 64 K to 334 W/cm^2 K at 76 K. This value is close to the calculated value (390 W/cm^2 K) including both the heat resistance at the film-substrate boundary (1000 W/cm^2 K) (Ref. 24) and in the substrate (637 W/cm^2 K) (cf. Fig. 5). It is higher than that of sample *B* (100–130 W/cm^2 K) (Ref. 8) and that obtained for $YBa_2Cu_3O_{7-\delta}$ superconducting films on the $SrTiO_3$ substrate (200 W/cm^2 K) by investigation of the hot-spot effect.[27] This may be due to the complicated heat transfer from film to bath, where the thermal resistance may appear at the film-substrate boundary, in the substrate, and at the boundary between the substrate and the sample holder [cf. Fig. 1(a)]. The inhomogeneities in the sample could also lead to an underestimated value of the heat-transfer coefficient in BS theory.[22]

An interesting experimental result observed both in low-T_c (Refs. 7,11–13) and high-T_c superconductors[6] is the magnetic-field dependence of the critical current I^*. In the $YBa_2Cu_3O_{7-\delta}$ system a scaling behavior for the temperature and magnetic-field dependence of the critical current density J^* was found:

$$J^*(T,H) = J^*(H)(1-T/T_{co})^{3/2} \tag{9}$$

with $J^*(H) = C/(1+H/H_0)^{\alpha}$, where T_{co}, H_0, α are fitting parameters, and C is the extrapolated value of the critical density at $T=0$ K and $B=0$ T. A power-law temperature dependence of the critical current I^* was also found in low-T_c superconductors.[28] Figure 6(a) shows that the critical current density J^* obtained here also displays a strong temperature and magnetic-field dependence. In fact, the data in Fig. 6(a) also scales with Eq. (9). The corresponding results for sample *A* are given in inset of Fig. 9(a), where $T_{co}=98$ K, $\mu_0H_0=1.35$ T, $\alpha=0.33$, and $C=5\times10^6$ A/cm^2 were extracted. For comparison, we also show the data of sample *B* in Fig. 9(a), where $T_{co}=92$ K, $\mu_0H_0=0.1$ T, $\alpha=0.37$, and $C=2.8\times10^7$ A/cm^2 were obtained. The symbols are experimental results, and the solid lines are calculated with Eq. (9).

This scaling behavior can be explained in the framework of the BS theory. Equations (4) and (6) predict that the temperature dependence of the critical current $I^*(T)$ will be determined by that of the inelastic scattering rate $1/\tau_{in}$ which can be fitted with a form of Eq. (8) in the range of high temperatures. Combining Eqs. (4), (6), and (8), the temperature dependence of the critical current I^* is proportional to $f=(1-T/T_c)^{3/4}\exp[3.52(1-T/T_c)^{1/2}/k_BT]$. As shown in Fig. 9(b) the function f can be expressed approximately in a power-law form with an exponent of 3/2 in the range of high

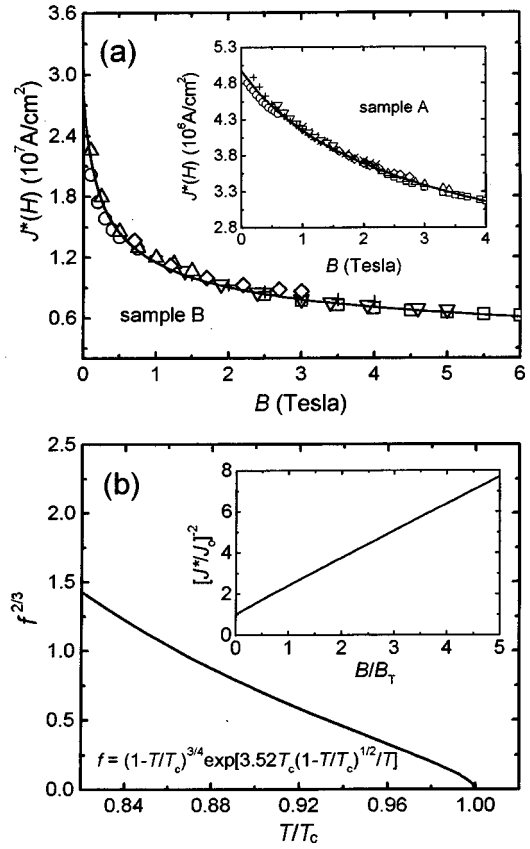

FIG. 9. (a) Scaling behavior of the experimentally obtained critical current density J^*, where $J^*(H)=J^*/(1-T/T_{co})^{3/2}$. The original experimental data of J^* of samples A and B are shown in Fig. 6(a) in this paper and Fig. 2(a) in Ref. 8, respectively. The solid lines are fits of $J^*(H)=C/(1+H/H_0)^{\alpha}$. The fitting parameters used are given in the text. (b) Theoretically predicted temperature and magnetic-field dependence of the critical current density [Eqs. (4) and (6)], where $f(T)\propto J^*(T)$. Equation (8) is used for the temperature dependence of $1/\tau_{in}$. In order for comparison with the experimentally observed scaling of Eq. (9), we plotted the results as $f^{2/3}$ versus T in a constant magnetic field and J^{*-2} versus B at a fixed temperature.

temperatures. Because J_0 is independent of the magnetic field, the relationship of I^* versus B is determined only by Eq. (4). As shown in the inset of Fig. 9(b), where $[J^*/J_0]^{-2}$ versus B/B_T is plotted, Eq. (4) can be simplified to $J^* \sim 1/(1+B/B_T)^{1/2}$ in a wide range of magnetic field. This is consistent with our experimental observation of $J^*(H)$ with an exponent α close to 1/2.

Although BS theory can account for the main features of our experimental data, a quantitative analysis would be expected to show some disparities between theory and experiment due to simplifying assumptions used. For example, Eq. (2) is valid at T not too far from T_c, where $T_q-T\ll T$ is expected. For high-T_c superconductors this temperature range could be large. Due to the high critical temperature and the short coherence length of the high-T_c superconductors, thermal fluctuations in these systems could be strong and lead to high dissipation at zero magnetic field. However, in this theory, the dissipation at zero magnetic field is presumed to be zero. Thus a disparity between theory and experiment could appear at low magnetic fields. It may be the reason why $P^*(=I^*V^*)$ does not vanish as B approaches zero. This may also be the origin of differing values for H_0 obtained in fits of the experimental data with Eq. (9). Equation (3) is derived for superconductors in the dirty limit with $l_0/\xi_0\ll 1$, where l_0 is the electron mean free path and ξ_0 is the BCS coherence length. However, most of the high-T_c superconductors belong to the moderate clean limit with l_0/ξ_0 larger than or close to 1.[29] Fortunately the main relationship between σ and E for the clean limit is the same as in Eq. (3).[30] The last possibility, as pointed out in Ref. 7, is the influence of pinning if the voltage jumps occur close to the vortex-glass state. There the total force opposing the vortex motion will be due to viscosity and pinning.

D. Anisotropy of voltage jumps

In $Bi_2Sr_2CaCu_2O_{8+\delta}$, the coherence length ξ_c in the c-axis direction can be smaller than the distance between the CuO_2 planes resulting in an extremely weak coupling between the layers. According to Kes *et al.*,[31] this material behaves as if the CuO_2 planes are decoupled and will show two-dimensional (2D) behavior. When a magnetic field is applied to this superconductor, only the c-axis component of the field (perpendicular to the CuO_2 planes) forms vortices and contributes to the dissipation, while the field component in the direction of the CuO_2 planes penetrates completely. A quantity Q, which depends on the magnetic field applied parallel to the c-axis direction, should show an angular dependence if the field is tilted from the c axis. The relationship between the value at an angle θ and the value at the c-axis direction ($\theta=0°$) will obey the following scaling law:

$$Q(B,T,\theta)=Q(B\cos\theta,T,0°), \tag{10}$$

where Q can represent the critical current I^* or the critical voltage V^* or even the entire I-V characteristic in these measurements. In Sec. III C we found that the I^* and V^* obtained in the c-axis direction of the sample depend on the magnetic field. Thus an angular dependence of I^* and V^* can be expected if Eq. (10) is applicable. As can be seen in Fig. 10, the scaling rule of Eq. (10) applies well to both the critical current I^* and the critical voltage V^*, where open squares are the values measured directly in a constant magnetic field with different tilt angles to the c axis and solid triangles represent the values calculated using Eq. (10) from the data taken at $\theta=0°$ and various fields.

J_0 and E_0 have no magnetic-field dependence, and should therefore have the same value at different angles. When Eqs. (4) and (5) are combined with Eq. (10) the same relationship between E^* and J^* is predicted in all magnetic-field directions. Thus, the data should collapse on an identical curve if we plot E^* versus J^* obtained at various angles. The corresponding results are given in Fig. 11(a). The symbols represent the experimental data obtained at three fixed temperatures 65, 71, and 76 K. The angles at which the data were taken are given in Fig. 11(b). The fits with Eqs. (4) and (5) for the data in $\theta=0°$ are given as solid lines in Fig. 11(a) and a good agreement between the theory and experiments can be found. According to BS theory, B_T is proportional to the time τ_{in} of the inelastic quasiparticle scattering. Therefore the anisotropy of τ_{in} could be investigated using flux-flow instability in an experiment specially designed to resolve the

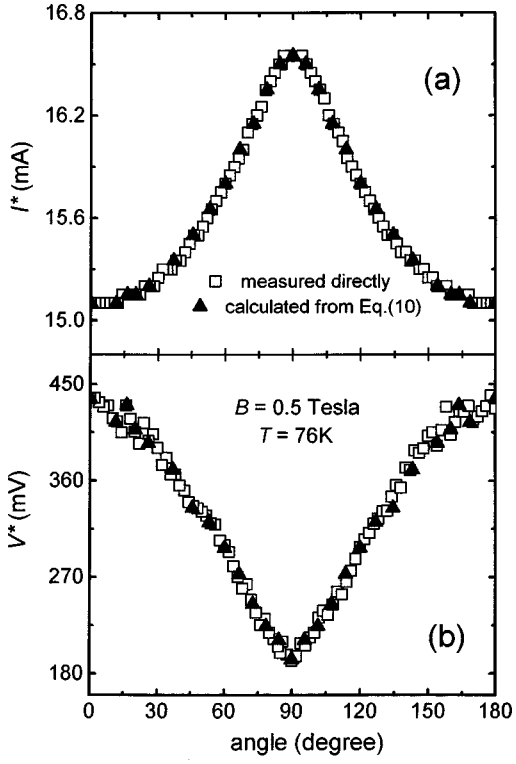

FIG. 10. Critical current I^* (a) and critical voltage V^* (b) at 76 K as a function of the angle θ between the magnetic field and the c axis of the film. Open squares represent the experimental data taken with $B=0.5$ T and $0°<\theta<180°$, solid triangles are the values calculated using Eq. (10) from the data taken at $\theta=0°$ and various B.

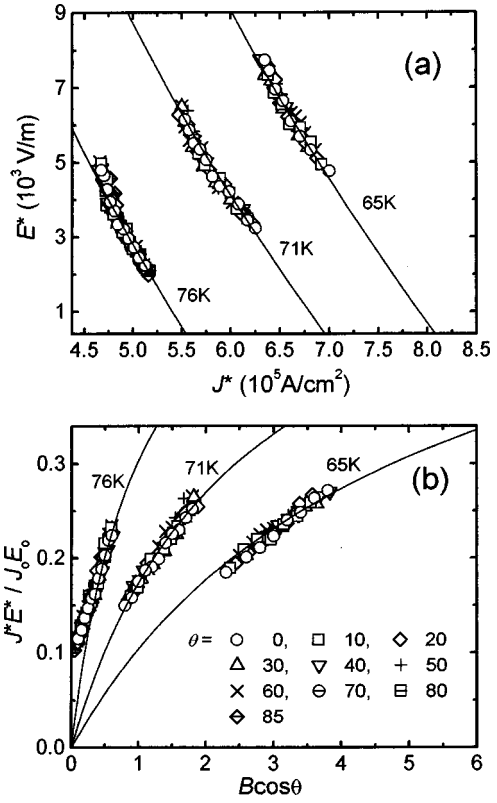

FIG. 11. (a) Relationship of the critical current density J^* and the critical electric field E^*. (b) Magnetic-field dependence of the dissipated power density. The symbols are the experimental data obtained at various magnetic-field orientations and the solid lines are calculated with Eqs. (4) and (5).

angular dependence of the characteristic magnetic field B_T. We use the same approach as used in Sec. III C to extract B_T in various magnetic-field orientations. Figure 11(b) shows the experimental data and the fitting results, where the experimental data were plotted as J^*E^*/J_0E_0 versus $B\cos\theta$ following the model of Kes *et al.* The collapse of the data obtained at a fixed temperature and various angles indicates that the dissipated power densities in various field directions are equal when the c-axis component of the field remains constant, as expected from Eq. (10). This result also demonstrates that the characteristic field B_T is independent of the direction of the magnetic field.

The above scaling behavior of the angular dependence of the critical current I^* and the critical voltage V^* could also be explained as the consequence of the angular dependence of the upper critical field B_{c2}. With a high anisotropy parameter both the quasi-2D model[32] and the anisotropic 3D model[33] predict a simple form for the anisotropy of the upper critical field with $H_{c2}(\theta)\approx H_{c2}(\theta=0°)/\cos\theta$. This leads to a strong angular dependence of the quasiparticle diffusion coefficient D ($\propto\cos\theta$) according to the relationship between D and H_{c2} ($\propto 1/D$).[22] Equations (6) and (7) in combination with the angle-independent E_0 and J_0 give the angular dependence of the characteristic field as $B_T=B_T(\theta=0°)/\cos\theta$. This indicates a strong anisotropy of the quasiparticle energy relaxation time $\tau_{\rm in}$ ($\propto 1/\cos\theta$). In those models one assumes that both the transverse and longitudinal components of the magnetic fields form the vortices. However, experiments such as Bitter patterns[34] show that the vortices are formed only by the c-axis component of the magnetic field. Recent muon-spin-rotation measurements provided microscopic evidence for the transparency of the CuO_2 (ab) planes of $Bi_2Sr_2CaCu_2O_{8+\delta}$ to magnetic fields.[35] For a model in which the vortex is formed only the c-axis component of the field, the experimentally determined upper critical field is a constant for $\theta=0°$.

In the above discussions we presumed that the anisotropy of the vortex instability originates from the intrinsic layer structure of this material. In the case of thin films, however, both theory and experiments demonstrated that a geometry effect could also induce an extrinsic anisotropy of some physical properties. For example, a simple cosine law for the angular dependence of the magnetic induction $B(\theta)$ in film has been predicted by considering a demagnetization effect;[36] A strong angular dependence of the critical current I_c (typically defined with a voltage criterion on the order of microvolts) was in fact observed in isotropic Nb-Ti films.[37] However $B(\theta)$ can only lead to a cosine law scaling of the physical properties like I_c in isotropic films where the upper critical field H_{c2} has no angular dependence. Combining the relation of B_{c2} and D, Eqs. (4) and (5) yields a magnetic-field dependence of J^* and E^* as a function of B/B_{c2}. If their anisotropies were caused by the demagnetization effect, the angular dependence of J^* and E^* should be scaled by $\cos^2\theta$, because B is proportional to $\cos\theta$ and B_{c2} is proportional to $1/\cos\theta$. This is not consistent with our experimental observation. The main difference between the models based on the 2D behavior of the superconductor and the demagnetization effect of the thin-film geometry is the orientation of

the vortices. In the first model the vortices are always in the c-axis direction with a constant B_{c2} for $\theta=0°$. In the second one the vortices change their orientations and the anisotropy of the upper critical field should be taken into account in analysis of the experimental data. On the other hand, the demagnetization effect is significant only in low magnetic field when the magnetic field cannot penetrate the sample. The demagnetization effect of $Bi_2Sr_2CaCu_2O_{8+\delta}$ films in our applied magnetic-field range should be neglected due to its strong type-II behavior and the comparatively small lower critical field B_{c1}. Despite the fact that anisotropy of the critical current I_c in Nb-Ti films is similar to that observed in some anisotropic high-T_c thin films, the 2D scaling has not yet been experimentally observed in isotropic films. In fact the 2D scaling behavior has also not been observed in $YBa_2Cu_3O_{7-\delta}$ thin films at either low[38] or high dissipation levels.[21] Measurements of $Bi_2Sr_2CaCu_2O_{8+\delta}$ thin films show a transition from 2D at low temperature, to 3D at temperatures close to T_c.[39] Data from measurements of thin $YBa_2Cu_3O_{7-\delta}/(Pr_xY_{1-x})Ba_2Cu_3O_{7-\delta}$ superlattices show that the 2D scaling is appropriate only when temperature T is high enough so that the PrYBCO layers become normal.[40] The temperature-dependent 2D scaling behavior for these two cases cannot be explained with the model based on the demagnetization effect of the film geometry.

In the limit of low vortex velocities, pinning plays an important role. For the anisotropy of the critical current I_c, for example, the same scaling law as Eq. (10) has been derived based on a mechanism of kink pinning.[41] The anisotropy of the critical current I_c reported in Ref. 37 might be induced by surface pinning. One facet of this work was designed to avoid the contributions from pinning by measuring the anisotropy of this superconductor in the limit of high vortex velocities. It is also of interest to study the orientation dependence of the flux-flow instability in isotropic superconducting films where no angular dependence of the critical current I^* and the critical voltage V^* is expected.

The 2D behavior of the $Bi_2Sr_2CaCu_2O_{8+\delta}$ superconductor was also investigated at low dissipation levels via measuring the angular dependence of the critical current I_c (Refs. 39,42) and of the magnetoresistivity in the low current limit.[43] To examine the consistence of our results at high flux-flow velocities with the previous reports in low dissipation levels, we measured the I-V characteristics for various magnetic-field directions with the same c-axis component at a fixed temperature. Figure 12 shows the corresponding experimental results obtained at 76 K for the c-axis component of a field $B\cos\theta=0.5$ T. As expected from the scaling law of Eq. (10), all I-V characteristics collapse on the same curve. This result indicates that dissipation at any level scales with the c-axis component of the magnetic field.

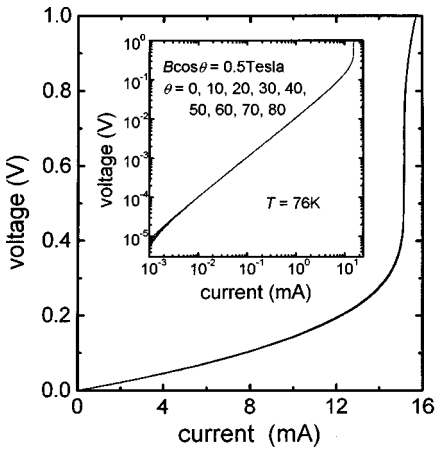

FIG. 12. Current-voltage characteristics taken with the same c-axis component of the field at a constant temperature. To examine the results at low dissipation levels, the data are plotted with a double-logarithmic scale in the inset.

IV. SUMMARIES

In conclusion, we have extended the investigation on the voltage instability in $Bi_2Sr_2CaCu_2O_{8+\delta}$ superconducting films. Voltage jumps were observed in I-V characteristics taken in a large range of temperatures and magnetic fields. The anisotropy of this voltage jump phenomenon has been studied by tilting the magnetic field from the c-axis direction of the sample. In all magnetic-field orientations the temperature and magnetic-field dependence of the critical current and critical voltage associated with the voltage jumps can be interpreted as due to a flux-flow instability with the influence of self-heating. Their angular dependence can be consistently described with a model based on the two-dimensional behavior of this superconductor.

ACKNOWLEDGMENTS

We would like to thank Q. B. Lu and R. Newsome for the critical reading of the manuscript. The project was financially supported by the SFB 262.

[1] A. I. Larkin and Yu. N. Ovchinnikov, Zh. Éksp. Teor. Fiz. **68**, 1915 (1975) [Sov. Phys. JETP **41**, 960 (1976)].
[2] A. E. Koshelev and V. M. Vinokur, Phys. Rev. Lett. **73**, 3580 (1994).
[3] O. Pla and F. Nori, Phys. Rev. Lett. **67**, 919 (1991).
[4] S. G. Doettinger, R. P. Huebener, R. Gerdermann, A. Kühle, S. Anders, T. G. Träuble, and J. C. Villegier, Phys. Rev. Lett. **73**, 1691 (1994).
[5] A. V. Samoilov, M. Konczykowski, N.-C. Yeh, S. Berry, and C. C. Tsuei, Phys. Rev. Lett. **75**, 4118 (1995).
[6] Z. L. Xiao and P. Ziemann, Phys. Rev. B **53**, 15 265 (1996).
[7] B. J. Ruck, J. C. Abele, H. J. Trodahl, S. A. Brown, and P. Lynam, Phys. Rev. Lett. **78**, 3378 (1997).
[8] Z. L. Xiao, P. Voss-de Haan, G. Jakob, and H. Adrian, Phys. Rev. B **57**, R736 (1998).
[9] G. Blatter, M. V. Feigel'man, V. B. Geshkenbein, A. I. Larkin, and V. M. Vinokur, Rev. Mod. Phys. **66**, 1125 (1994).
[10] J. W. Bremer and V. L. Newhouse, Phys. Rev. **116**, 309 (1959).
[11] L. E. Musienko, I. M. Dmitrenko, and V. G. Volotskaya, Pis'ma Zh. Éksp. Teor. Fiz. **31**, 603 (1980) [JETP Lett. **31**, 567 (1980)].
[12] W. Klein, R. P. Huebener, S. Gauss, and J. Parisi, J. Low Temp. Phys. **61**, 413 (1985).

[13] Y. Ando, H. Kubota, S. Tanaka, M. Aoyagi, H. Akoh, and S. Takada, Phys. Rev. B **47**, 5481 (1993).
[14] W. Henderson, E. Y. Andrei, M. J. Higgins, and S. Bhattacharya, Phys. Rev. Lett. **77**, 2077 (1996).
[15] A. VI. Gurevich and R. G. Mints, Rev. Mod. Phys. **59**, 941 (1987).
[16] Y. Matsuo, T. Nojima, Y. Kuwasawa, E. Majkova, and S. Luby, Physica C **277**, 138 (1997); R. Tidecks and G. Slama, Z. Phys. B **37**, 103 (1980).
[17] S. G. Doettinger, R. P. Huebener, and A. Kühle, Physica C **251**, 285 (1995).
[18] S. G. Doettinger, S. Kittelberger, R. P. Huebener, and C. C. Tsuei, Phys. Rev. B **56**, 14 157 (1997).
[19] M. Xu, D. L. Shi, and R. F. Fox, Phys. Rev. B **42**, 10 773 (1990), and references therein.
[20] Z. L. Xiao and P. Ziemann, Physica C **282-287**, 2363 (1997).
[21] Z. L. Xiao and P. Ziemann, Z. Phys. B **104**, 451 (1997).
[22] A. I. Bezuglyj and V. A. Shklovskij, Physica C **202**, 234 (1992).
[23] P. Wagner, F. Hillmer, U. Frey, H. Adrian, T. Steinborn, L. Ranno, A. Elschner, I. Heyvaert, and Y. Bruynseraede, Physica C **215**, 123 (1993).
[24] S. K. Gupta, P. Berdahl, R. E. Russo, G. Briceno, and A. Zettl, Physica C **206**, 335 (1993).
[25] Milind N. Kunchur, David K. Christen, Charles E. Klabunde, and Julia M. Phillips, Phys. Rev. Lett. **72**, 752 (1994).
[26] W. J. Skocpol, M. R. Beasley, and M. Tinkham, J. Appl. Phys. **45**, 4054 (1974).
[27] Z. L. Xiao, E. Y. Andrei, and P. Ziemann, Phys. Rev. B **58**, 11 185 (1998).
[28] G. Dharmadurai and B. A. Ratnam, Phys. Lett. **67A**, 49 (1978).
[29] S. J. Hagen, A. W. Smith, M. Rajeswari, J. L. Peng, Z. Y. Li, R. L. Greene, S. N. Mao, X. X. Xi, S. Bhattacharya, Qi Li, and C. J. Lobb, Phys. Rev. B **47**, 1064 (1993).
[30] S. G. Doettinger, R. P. Huebener, S. Kittelberger, and C. C. Tsuei, Europhys. Lett. **33**, 641 (1996).
[31] P. H. Kes, J. Aarts, V. M. Vinokur, and C. J. van der Beek, Phys. Rev. Lett. **64**, 1063 (1990).
[32] W. E. Lawrence and S. Doniach, in *Proceedings of the 12th International Conference on Low Temperature Physics, Kyoto, Japan, 1970*, edited by E. Kanda (Kiegaku, Tokyo, 1971), p. 361; E. Silva, S. Sarti, M. Guira, R. Fastampa, and R. Marcon, Phys. Rev. B **55**, 11 115 (1997).
[33] M. Tinkham, *Introduction to Superconductivity* (McGraw-Hill, New York, 1996).
[34] C. A. Bolle, P. L. Gammel, D. G. Grier, C. A. Murray, D. J. Bishop, D. B. Mitzi, and A. Kapitulnik, Phys. Rev. Lett. **66**, 112 (1991).
[35] W. J. Kossler, Y. Dai, K. G. Petzinger, A. J. Greer, D. Ll. Williams, E. Koster, D. R. Harshman, and D. B. Mitzi, Phys. Rev. Lett. **80**, 592 (1998).
[36] H. Theuss, T. Becker, and H. Kronmüller, Physica C **233**, 179 (1994).
[37] G. Stejic, A. Gurevich, E. Kadyrov, D. Christen, R. Joynt, and D. C. Larbalestier, Phys. Rev. B **49**, 1274 (1994).
[38] B. Roas, L. Schultz, and G. Saemann-Ischenko, Phys. Rev. Lett. **64**, 479 (1990).
[39] P. Schmitt, P. Kummeth, L. Schultz, and G. Saemann-Ischenko, Phys. Rev. Lett. **67**, 267 (1991).
[40] Q. Li, C. Kwon, X. X. Xi, S. Bhattacharya, A. Walkenhorst, T. Venkatesan, S. J. Hagen, W. Jiang, and R. L. Greene, Phys. Rev. Lett. **69**, 2713 (1992).
[41] V. L. Pokrovsky, I. Lyuksyutov, and T. Nattermann, Phys. Rev. B **46**, 3071 (1992).
[42] G. Jakob, M. Schmitt, Th. Kluge, C. Tome-Rosa, P. Wagner, Th. Hahn, and H. Adrian, Phys. Rev. B **47**, 12 099 (1993).
[43] H. Raffy, S. Laddi, O. Laborde, and P. Monceau, Phys. Rev. Lett. **66**, 2515 (1991).